

Sensing T-violating nuclear moments of paramagnetic ions in crystals

Aleksandar Radak,¹ Mingyu Fan,¹ Bassam Nima,¹ Yuiki Takahashi,² and Amar Vutha¹

¹*Department of Physics, University of Toronto, Toronto ON M5S 1A7, Canada*

²*Division of Physics, Mathematics, and Astronomy,
California Institute of Technology, Pasadena, California 91125 USA*

(Dated: March 27, 2026)

Precision measurements of time-reversal (T) symmetry violating moments probe physics beyond the Standard Model. We show that precision spectroscopy of paramagnetic lanthanide and actinide ions doped into noncentrosymmetric crystals offers a promising platform for extending the sensitivity of searches for T-violation in nuclear physics. The unpaired valence electron in these ions allows the engineering of highly-coherent hyperfine transitions that are insensitive to magnetic fields, yet highly sensitive to new physics. These systems also provide other advantages for new physics searches, including large numbers of ions that can be measured in doped crystals, strong electric polarization of the ions by the crystal fields, enhancement of T-violating nuclear moments in nonspherical nuclei, and accurate comagnetometers generated by crystal symmetry. We estimate the new physics sensitivity of these proposed systems to be two orders of magnitude better than existing constraints.

The Standard Model of particle physics is known to be incomplete. In particular, new sources of time-reversal (T) symmetry violation are needed to explain the abundance of matter over antimatter in the observable universe. Precision measurements of parity (P)-odd T-odd moments in atomic and molecular systems have emerged as powerful probes for physics beyond the Standard Model, providing access to new physics at energy scales exceeding those in collider experiments [1].

Atomic ions in crystals, whose internal quantum states can be optically controlled using lasers, are attracting interest as a promising new platform for T-violation measurements [2–5]. These solid-state systems are particularly amenable for measuring symmetry-violating nuclear moments: the nuclei are significantly shielded against perturbations from the crystal lattice which enables measurements with long coherence times, whereas optical control and readout of nuclear spins allow high-precision symmetry-resolved measurements using large ensembles of nuclei.

In a crystal with noncentrosymmetric doping sites, such as yttrium orthosilicate (YSO), the dopant ions are in positions where parity is locally broken. The ions can therefore have large static electric polarization at equilibrium. The electrons in such a polarized ion create field gradients that interact with T-violating nuclear moments, leading to measurable P-odd T-odd perturbations in the hyperfine structure of the ion [4]. The overall crystal symmetry, on the other hand, produces sub-ensembles of ions that are polarized in opposite directions. These ion sub-ensembles exhibit identical sensitivities to magnetic fields, but opposite sensitivities to T-violating effects. Thus, comparisons between these “comagnetometer” ensembles allow experiments to cleanly isolate new physics signals from spurious effects produced by magnetic fields, as demonstrated in Refs. [6, 7].

Lanthanide and actinide ions are ideal dopants in such

crystals. They have valence electrons in f orbitals that are shielded from the lattice by outer s or p electrons, so that the optical transitions of the valence electrons are only weakly perturbed by the crystal fields. As a result, narrow optical transitions with long coherence times are observed, which can be used to achieve efficient preparation and low-noise readout of hyperfine states [8]. Furthermore, some lanthanides and actinides have isotopes with significant nuclear nonsphericity, which enhances the sensitivity of these isotopes to hadronic T-violation [3, 9].

Experiments using diamagnetic lanthanide ions in noncentrosymmetric crystals have previously been used to perform sensitive searches for new physics [7]. Here, we show that hyperfine transitions in *paramagnetic* ions can be engineered to become insensitive to magnetic fields, yet retain high sensitivity to new physics. We propose $^{167}\text{Er}^{3+}$, $^{229}\text{Th}^{3+}$, $^{233}\text{U}^{3+}$, and $^{235}\text{U}^{3+}$ ions doped in YSO as representative candidate systems for measuring P-odd T-odd nuclear moments, such as the nuclear Schiff moment (NSM) and the nuclear magnetic quadrupole moment (MQM). The above isotopes exhibit collective octupole or quadrupole modes that enhance their sensitivity to new physics [10]. Optical transitions in these ions can be used for efficient state preparation and readout as in the diamagnetic case. Importantly, in addition, these systems can be engineered to have magnetic-field-insensitive hyperfine transitions.

We project that a 10-day measurement with such systems can probe T-violating physics at a statistical sensitivity that is significantly better than current T-violating parameter limits, probing new particles at an energy scale ~ 100 TeV. In addition, the same measurement can also set improved broadband bounds on axionlike particle (ALP) dark matter. Outside of searches for nuclear T-violation, such transitions in, e.g., ^{229}Th doped solids, may be useful for applications such as timekeeping and

searches for the variability of fundamental constants.

Hyperfine structure — When lanthanide or actinide atoms are doped into a YSO crystal, they substitute for yttrium ions and typically stabilize in a trivalent charge state. The effective Hamiltonian for the nuclear and electronic degrees of freedom in these ions can be written as

$$H = H_{\text{FI}} + H_{\text{CF}} + H_{\text{HF}}, \quad (1)$$

where H_{FI} is the free ion Hamiltonian, H_{CF} represents the interaction with the crystal field, and H_{HF} contains hyperfine and magnetic interactions [8]. The energy scales involved in this Hamiltonian are schematically illustrated in Fig. 1. Electronic transitions between eigenstates of the free ion typically occur at optical frequencies. Within each free ion electronic state, the interaction with the crystal breaks rotational symmetry and splits each electronic state by lifting the degeneracy of its magnetic levels. Each electronic state of paramagnetic systems, with a total electronic angular momentum of a half integer, forms fine-structure Kramers pairs under the influence of H_{CF} [11]. In the ground electronic state of the ion, denoted as Z , the fine-structure Kramers pairs are denoted Z_1, Z_2, \dots in increasing order of energy. For an excited state of the ion, denoted as Y , the fine-structure Kramers pairs are labelled Y_1, Y_2, \dots in increasing order of energy. Typical transitions between adjacent Kramers pairs occur in the THz frequency range.

At cryogenic temperatures (at $\lesssim 4$ K as typical in experiments), only the lowest electronic Kramers pair Z_1 is appreciably populated at thermal equilibrium. In this regime, the electronic degree of freedom can be described as an effective spin-1/2 system with the spin operator \vec{S} [12, 13]. The isotopes discussed here have half-integer nuclear spin ($I = 5/2$ for ^{229}Th and ^{233}U , and $I = 7/2$ for ^{167}Er and ^{235}U). Combining the electronic and nuclear degrees of freedom, there are $N = 2(2I + 1)$ hyperfine states within the Z_1 manifold.

The hyperfine and Zeeman Hamiltonian for this manifold is [14]

$$H_{\text{HF}} = \mathbf{A}_{ij} \mathbf{S}_i I_j + \mathbf{Q}_{ij} I_i I_j + \mu_B \mathbf{g}_{ij} \mathbf{S}_i \mathcal{B}_j - \mu_N \mathbf{g}_N \delta_{ij} I_i \mathcal{B}_j. \quad (2)$$

The indices $i, j \in \{x, y, z\}$ and repeated indices are summed over. The hyperfine coupling tensor is \mathbf{A}_{ij} , the nuclear quadrupole interaction tensor is \mathbf{Q}_{ij} , and \mathbf{g}_{ij} is the electronic g-tensor. Here \mathbf{g}_N is the nuclear g-factor, μ_B (μ_N) is the Bohr (nuclear) magneton, and \mathcal{B}_j is the j -th component of the laboratory magnetic field. We denote eigenstates of H_{HF} as $|0\rangle, \dots, |N-1\rangle$ in order of increasing energy.

P-odd T-odd nuclear moments generated by physics beyond the Standard Model introduce further hyperfine interactions. The effective Hamiltonians describing the interaction of the nuclear Schiff moment (NSM)

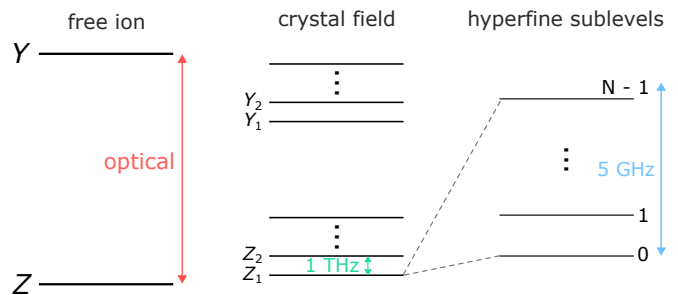


FIG. 1. Schematic of the energy level structure of paramagnetic ions in YSO. The degeneracy of electron spin sub-levels in the Z and Y electronic states is lifted by the interactions with the crystal. An optical transition between the two electronic states can be used for controlling and probing the ions. Each of the energy levels Z_i, Y_j are doubly-degenerate Kramers pairs. Within each of these is a manifold of hyperfine states.

$\vec{S} = \mathcal{S}\vec{I}/|I|$ and nuclear magnetic quadrupole moment (MQM) \mathcal{M} [15–17] are

$$H_{\text{NSM}} = \mathcal{W}_S \mathcal{S} \frac{\vec{I}}{|\vec{I}|} \cdot \hat{n} \quad (3)$$

and

$$H_{\text{MQM}} = -\mathcal{W}_M \mathcal{M} \vec{I}_j \mathbf{S}_i n_j, \quad (4)$$

where \mathcal{W}_S (\mathcal{W}_M) is a coefficient that characterizes the interaction of the NSM (MQM) with electrons in the ion. The unit vector \hat{n} is the direction of electric polarization of the ion in the crystal. Here, \vec{I}_j is the rank 2 tensor operator $\vec{I}_j = \frac{1}{2I(2I-1)} \left[I_i I_j + I_j I_i - \frac{2}{3} \delta_{ij} I(I+1) \right]$.

In the YSO crystal (C_2/c space group), there are two types of Y^{3+} sites with different coordination numbers. We restrict our attention to the better-characterized “site 1” ions that have 7 nearest neighbor oxygen ions. Ions that substitute for Y^{3+} in site 1 have four possible configurations that are related by two symmetries: a parity transformation (denoted as $\hat{\Pi}$), and a 180° rotation around the \mathbf{b} dielectric axis of the crystal (denoted as $\hat{\Sigma}$) [6]. The $\hat{\Pi}$ transformation relates two sub-ensembles of ions that have opposite electric polarization unit vector \hat{n} . We label these sub-ensembles of ions by the quantity $\pi \equiv \text{sign}(\hat{n} \cdot \hat{x}) = \pm 1$, where we align the unit vectors in the lab-frame coordinate system ($\hat{x}, \hat{y}, \hat{z}$) with the dielectric axes of the crystal, $\mathbf{D}_1, \mathbf{D}_2$, and \mathbf{b} , respectively.

As both H_{NSM} and H_{MQM} are dependent on the polarization direction \hat{n} , we can isolate P-odd T-odd energy shifts by measuring the *difference* of hyperfine resonance frequencies between the $\pi = \pm 1$ sub-ensembles. In order to distinguish oppositely polarized ions, a lab electric field $\vec{\mathcal{E}}$ (~ 100 V/cm) can be applied to the crystal, which interacts with the atomic dipole moment dif-

ference between electronic states $\Delta D\hat{n}$ and generates an ion-polarization-dependent frequency shift $\Delta D\hat{n}\cdot\hat{\mathcal{E}}$. This optical frequency shift allows separately addressing the two sub-ensembles. Since the $\pi = \pm 1$ sub-ensembles have identical magnetic interactions but different new physics interactions, comparison between hyperfine resonances in these ions enables the separation of energy shifts due to new physics from those due to spurious magnetic fields, as demonstrated in Ref. [6].

NTSC transitions — When lanthanide or actinide ions are doped in a crystal such as YSO, at special values of the lab magnetic field (called “ZEFOZ points”), there exist pairs of hyperfine sublevels with equal magnetic moments along all three axes [18–20]. A transition between such a pair of sublevels therefore becomes first-order insensitive to magnetic field fluctuations. In electron-spin-diamagnetic ions (such as Eu^{3+} that was used in Refs. [6, 7]), all ZEFOZ points coincide with zero sensitivity to new physics. Therefore there is no practical advantage to using such ions at ZEFOZ points for T-violation search experiments. Crucially, however, in *electron-spin-paramagnetic* ions there exists a subset of ZEFOZ points where the system retains high sensitivity to P-odd T-odd new physics. We refer to these as nuclear T-violation-sensitive clock (NTSC) transitions.

The concept of engineering transitions that are insensitive to electromagnetic field fluctuations, but remain sensitive to T-violation, has been recently proposed [21] and demonstrated in polar molecules [22]. NTSC transitions for ions in crystals can be understood along similar lines. The essential idea is that the three terms in the hyperfine Hamiltonian – the Zeeman, NSM, and MQM terms – are each dependent on different combinations of \vec{S} and \vec{I} . The Zeeman effect is dominated by $g_{ij}\mathcal{S}_i\mathcal{B}_j$, whereas the NSM depends on $\vec{I}\cdot\hat{n}$ and the MQM on $\mathcal{S}_i n_j \mathcal{I}_{ij}$. Thus, two hyperfine states with identical magnetic moments must have nearly the same expectation values of electron spin projections along all axes; however, their nuclear spin vectors can have different orientations. Therefore, transitions between two such states can be insensitive to magnetic fields to first order, while remaining sensitive to the NSM and MQM.

Using the hyperfine parameters of an electron-spin-paramagnetic ion, ^{167}Er , located at site 1 in YSO [14] as an example, we identify four NTSC transitions occurring at $|\mathcal{B}| \lesssim 1$ T that have high sensitivity to nuclear T-violation while also having appreciable transition dipole moments. These transitions are shown in Fig. 2. The coherence time of these transitions is estimated as approximately 0.1 s (see the Appendix). Furthermore, different NTSC transitions have different sensitivities to the NSM and MQM, so that comparison of measured energy shifts across a set of NTSC transitions can measure the NSM and MQM individually. Additionally, at an NTSC point, all transitions other than the NTSC transition have large

magnetic field sensitivities of ~ 10 MHz / G. These transitions can therefore be used to detect and correct magnetic field imperfections that could generate systematic errors, as has been demonstrated in molecules [22]. Combined with the comagnetometry method demonstrated in Ref. [6], the overall experimental platform has extremely robust protection against systematic errors while maintaining high sensitivity to T-violation.

The existence of NTSC transitions is a generic and robust feature of electron-spin-paramagnetic ions in crystals such as YSO. To verify this fact, we numerically vary the magnitude of \mathcal{Q}_{ij} and \mathcal{A}_{ij} tensors of $^{167}\text{Er}:\text{YSO}$ up and down by a factor of two. Over this entire parameter range, there exist NTSC transitions with comparable coherence time, as well as similar NSM and MQM sensitivities, as the transitions shown in Fig. 2. All the paramagnetic lanthanide and actinide ions considered here (Er^{3+} , Th^{3+} and U^{3+}) have the same form of hyperfine Hamiltonian as Eq. 2, and thus they generically exhibit NTSC transitions.

Measurement protocol — To conduct precision searches of T-violating nuclear moments using these NTSC transitions, we propose a protocol with the essential idea similar to that for $\text{Eu}:\text{YSO}$ [6]– state preparation, radio-frequency (rf) spectroscopy, and comagnetometry readout. State preparation and detection rely on the optical transition between the ground Z_1 level and the excited Y_1 level.

Similar to the measurement scheme used in Ref. [7], a chosen spectral class of ions is initially prepared in a hyperfine state $|i\rangle$ using spectral holeburning and optical pumping. Next, the hyperfine transition energy between $|i\rangle$ and a second sublevel $|f\rangle$ is probed using rf Ramsey spectroscopy. Finally, the population remaining in $|i\rangle$ is optically detected.

During the detection, a laboratory electric field is applied to the crystal, which shifts the optical transition frequency in opposite directions for $\pi = \pm 1$ ions, as demonstrated in Ref. [6]. Thus the population remaining in $|i\rangle$ for each polarization of ion can be distinguished, allowing simultaneous measurements of the $|i\rangle \rightarrow |f\rangle$ transition frequency across the $\pi = \pm 1$ sub-ensembles. The sum of the two resonance frequencies measured in $\pi = \pm 1$ sub-ensembles only contains the Zeeman shift, whereas their difference isolates just the T-violating terms from the NSM and MQM.

This measurement scheme can be applied to all the systems considered here ($\text{Er}:\text{YSO}$, $\text{Th}:\text{YSO}$ and $\text{U}:\text{YSO}$). Er^{3+} has a $^4I_{15/2} \rightarrow ^4I_{13/2}$ transition at 1536 nm in YSO [23]. Th^{3+} has a $^2F_{5/2} \rightarrow ^2F_{7/2}$ optical transition at ~ 2 μm [24]. Optical spectroscopy of $\text{U}^{3+}:\text{LaCl}_3$ has identified the $^4I_{9/2} \rightarrow ^4F_{3/2}$ transition at 1.4 μm [25]. All these intraconfigurational transitions are only weakly allowed via magnetic dipole ($M1$) transitions or through mixing effects of the crystal electric field, leading to narrow optical linewidths [26, 27] that are convenient for

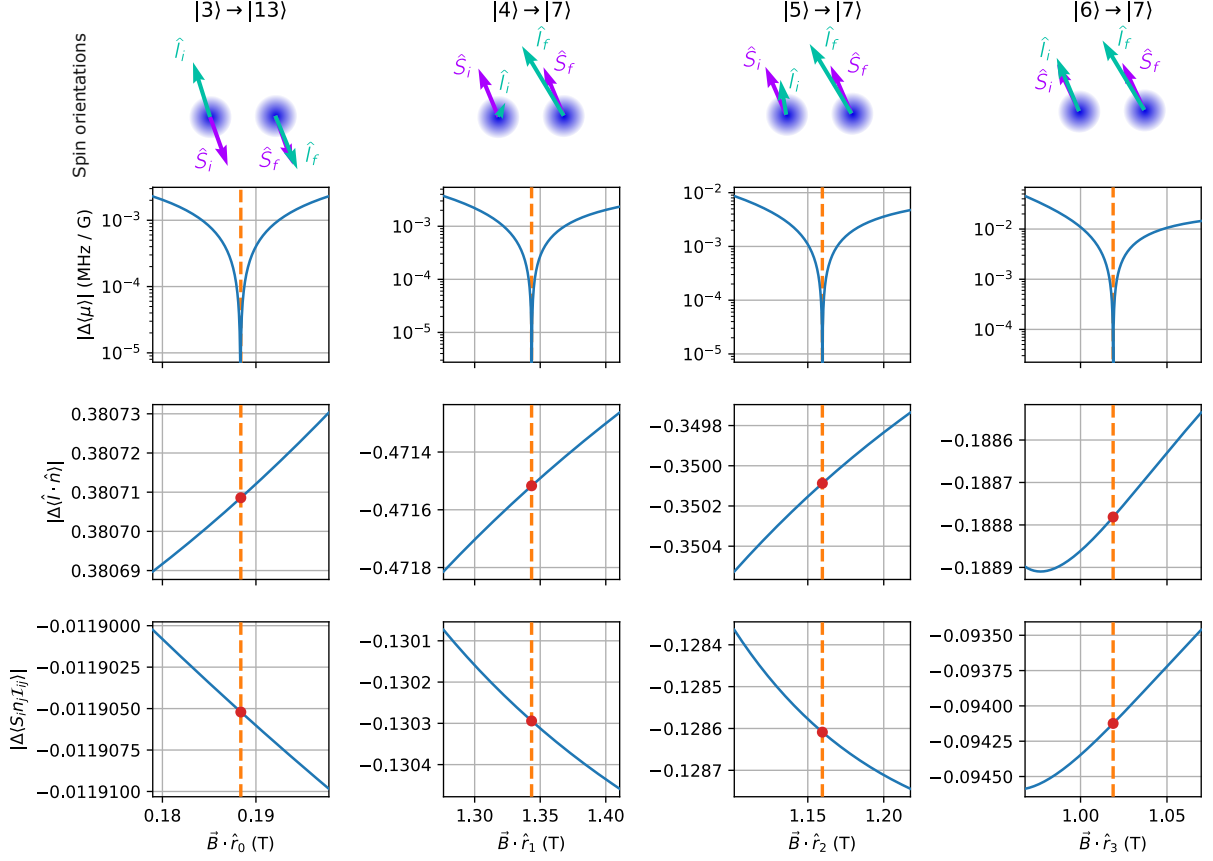


FIG. 2. Example NTSC transitions for site 1 ions of $^{167}\text{Er}:\text{YSO}$. Each column represents a transition $|i\rangle \rightarrow |f\rangle$, with the hyperfine sublevels labeled in the order of low to high energy. The magnitude of the magnetic field is varied along the direction of the NTSC magnetic field for each transition (\hat{r}_k for transitions labeled by $k \in \{0, 1, 2, 3\}$). The top row shows the expectation values of the electron spin projection $\hat{S} = \vec{S}/|\vec{S}|$ and the nuclear spin projection $\hat{I} = \vec{I}/|\vec{I}|$ of initial and final states at the NTSC magnetic fields in the $x - y$ plane. The electron spins of the two states have nearly identical expectation values which ensures that both states have identical magnetic moments, while the nuclear spins in these states have different expectation values. The magnetic field sensitivity, the NSM sensitivity, and the MQM sensitivity are shown as a function of the magnetic field. The NTSC magnetic fields are labeled as orange dashed lines, and the NSM and MQM sensitivities at the NTSC magnetic field are denoted by red dots.

hyperfine state-preparation and readout.

The radioactive isotopes ^{229}Th , ^{233}U , and ^{235}U have half-lives of more than thousands of years, suitable to be incorporated in macroscopic crystals. Recently, optical excitation of ^{229}Th ions in crystals has been achieved [28–30], and radioactive crystal production techniques have been demonstrated [31]. These developments confirm that radioactive dopants can be stably embedded in crystals for precision measurements, removing technical barriers to nuclear T-violation measurements with these nuclei. While neither Th or U have been doped into YSO, the isoelectronic lanthanides Ce and Nd have been doped into YSO and characterized [32, 33]. Moreover, trivalent uranium-doped crystals have been produced for spectroscopy, including $\text{U}:\text{CaF}_2$ and $\text{U}:\text{LiYF}_4$ [34, 35]. Like YSO, these crystals may host other trivalent lanthanide ions, for instance, Pr, Eu, Ho, and Yb, indi-

cating that U^{3+} may be doped into YSO [36–43]. The two isotopes $^{233,235}\text{U}$ have different intrinsic sensitivity to hadronic T-violation, and therefore comparing experimental measurements between these isotopes offers yet another means for stringent separation of systematic errors from genuine new physics effects.

Expected sensitivity — The attainable sensitivity of the proposed systems to T-violating physics can now be evaluated. The sensitivity of the NTSC transition frequency is

$$\Delta f = \frac{1}{2\pi T_{\text{coh}} \text{SNR} \sqrt{N}} = 65 \text{ nHz}. \quad (5)$$

In the above estimate we use a coherence time of $T_{\text{coh}} = 0.14 \text{ s}$, as calculated for the $|4\rangle \rightarrow |7\rangle$ NTSC transition at 1.343 T for $^{167}\text{Er}:\text{YSO}$ (see the Appendix). We expect similar coherence times in crystals doped with Th

and U isotopes. The signal-to-noise ratio $\text{SNR} = 10^4$ is based on the estimated photon shot noise during spectroscopy (see the Appendix). We assume the sum of the state preparation and detection times to be equal to the coherence time, such that each measurement takes 0.28 s and $N = 3 \times 10^6$ measurements can be made in ten days.

We use Eqs. 3 and 4 to convert Δf to the nuclear moment sensitivities. The electronic enhancement coefficients in YSO have been estimated to be an order of magnitude lower than those for polar molecules [9, 44, 45], and therefore we assume reference values of $\mathcal{W}_S \sim 100$ kHz/(e fm³) and $\mathcal{W}_M \sim 1$ MHz/(e fm²).

We use the NSM and MQM sensitivity factors, $\langle \hat{I} \cdot \hat{n} \rangle = -0.47$ and $\langle S_{ij} n_j \mathcal{I}_{ij} \rangle = -0.13$ respectively, calculated for the $|4\rangle \rightarrow |7\rangle$ NTSC transition in ¹⁶⁷Er:YSO. The statistical sensitivity of an experiment to hadronic T-violation effects can now be expressed in terms of the QCD θ parameter, which parametrizes the strength of a T-violating new physics term. These sensitivities are shown in Table I. The calculated sensitivities of the proposed solid-state systems, $\delta\theta \sim 10^{-12}$, exceed the current hadronic T-violation bound $|\theta| < 10^{-10}$ set by the Hg and neutron electric dipole moment experiments [46, 47]. Furthermore, by analyzing temporal oscillations in θ derived from measurements of the NSM and MQM, we may search for ALP dark matter (e.g., [7]). With the estimated experimental sensitivity to a possible NSM of ²³⁵U, we can constrain the ALP-gluon interaction strength between ALP masses m_a of 5×10^{-21} eV and 7×10^{-15} eV at a sensitivity of $4 \text{ GeV}^{-1} \times m_a / (1 \text{ eV})$. This is an improvement of 2 to 4 orders of magnitudes over the previous limits set by T-violating moment experiments [48–50].

In conclusion, we summarize the advantages offered by paramagnetic lanthanide and actinide ions doped in noncentrosymmetric crystals for probing P-odd T-odd physics beyond the Standard Model. These systems combine nonspherical nuclei, with high intrinsic sensitivity to hadronic T-violating physics, together with noncentrosymmetric crystal sites that offer large enhancements of the nuclear moments generated by T-violation. The proposed systems possess robust means to reject systematic errors using (a) comagnetometers generated by crystal symmetries, and (b) magnetically-insensitive transitions that remain highly sensitive to T-violating new physics. We estimate that measurements of the nuclear Schiff moment and magnetic quadrupole moment using these solid-state systems can significantly improve the sensitivity of searches for nuclear T-violation, enabling tabletop-scale probes of new physics at the 100 TeV energy scale.

Acknowledgment.— M.F. acknowledges funding from a CQIQC Postdoctoral Fellowship. Y.T. was supported by an IQIM Eddleman Fellowship and the Masason Foundation. This project was enabled by support from NSERC

(grant no. SAPIN-2021-00025).

Appendix A: List of NTSC transitions in ¹⁶⁷Er:YSO

We discuss the new physics sensitivities of the calculated NTSC transitions in site 1 of ¹⁶⁷Er:YSO as a prototypical example, since detailed spectroscopy data is available for this ion [14]. The time-varying magnetic field at the position of Er³⁺ ions is dominated by fluctuations in the orientations of ⁸⁹Y spins in the crystal, which reduce the coherence time of the transitions. As the linear Zeeman effect is absent, the coherence time of an NTSC transition at frequency f_0 is related to the quadratic Zeeman shift as [51]

$$\frac{1}{\pi T_2} = K_{ij} \Delta \mathcal{B}_i \Delta \mathcal{B}_j. \quad (6)$$

Here $\Delta \mathcal{B} \approx 8 \mu\text{T}$ is the estimated root-mean-squared magnetic field fluctuation due to the nearby Y nuclear spins [51], and $K_{ij} = \frac{\partial^2 f_0}{\partial \mathcal{B}_i \partial \mathcal{B}_j}$ is the curvature of the transition frequency with magnetic field. We assume that the magnetic field fluctuations are along the principal axis of K_{ij} with the largest magnitude eigenvalue. We list the calculated coherence times of NTSC transitions in Table II along with their NSM and MQM sensitivities.

Appendix B: Optical spectroscopy signal-to-noise ratio

The $f-f$ transitions considered in this work are either $M1$ transitions or weakly allowed $E1$ transitions induced by the crystal field, with typical $E1$ oscillator strengths of $f_{\text{osc}} \sim 10^{-7}$ [52]. With an incident laser of electric field amplitude \mathcal{E}_0 , the Rabi frequency is $\Omega = d\mathcal{E}_0/\hbar$, where $d = \sqrt{3\hbar e^2 f_{\text{osc}}}/(2m_e \omega_0)$ is the transition electric dipole moment. Here m_e is the electron mass and ω_0 is the frequency of the optical transition.

Using realistic experimental parameters (transition wavelength $\lambda = c/(2\pi\omega_0) \approx 1 \mu\text{m}$ and laser intensity $I = \epsilon_0 c \mathcal{E}_0^2/2 = 1 \mu\text{W mm}^{-2}$), we obtain

$$\Omega = 2\pi \times 640 \text{ Hz} \sqrt{\frac{\lambda}{1 \mu\text{m}} \frac{I}{1 \mu\text{W mm}^{-2}} \frac{10^{-7}}{f_{\text{osc}}}}. \quad (7)$$

To prevent excess optical pumping during spectroscopy, we excite less than 10% of the population, resulting in a maximum optical detection time of $T_{\text{detect}} \approx 25 \mu\text{s}$. With a crystal cross sectional area $A = 1 \text{ mm}^2$, the number of photons detected is $N_{\text{photons}} = IA T_{\text{detect}}/(\hbar\omega_0) = 1.3 \times 10^8$, giving a photon shot-noise-limited $\text{SNR} = \sqrt{N_{\text{photons}}} = 1.1 \times 10^4$ for a spectral feature of optical depth ~ 1 .

TABLE I. Comparison of systems of different isotopes doped in YSO. Columns are species; Rows list nuclear spin I , the NSM \mathcal{S} [10], the MQM \mathcal{M} [10], and the estimated statistical sensitivities of the QCD θ parameter $\delta\theta_{\text{NSM}}$ and $\delta\theta_{\text{MQM}}$, given the spectroscopy sensitivity estimated in Eq. 5.

Isotope	I	\mathcal{S} ($\theta \times e \cdot \text{fm}^3$)	\mathcal{M} ($\theta \times e \cdot \text{fm}^2$)	$\delta\theta_{\text{NSM}}$	$\delta\theta_{\text{MQM}}$
^{167}Er	7/2	^a	0.13	-	4×10^{-12}
^{229}Th	5/2	1.2	0.09	1.2×10^{-12}	6×10^{-12}
^{233}U	5/2	0.44	0.09^b	3×10^{-12}	6×10^{-12}
^{235}U	7/2	1.9	0.09	7×10^{-13}	6×10^{-12}

^aThe NSM of ^{167}Er is on the order of $\sim 10^{-3}\theta \times e \cdot \text{fm}^3$ as it does not have octupolar enhancement, so it is not listed.

^bFor ^{233}U we use the MQM of ^{235}U since their masses are very similar.

TABLE II. Selected NTSC transition frequencies f_0 , NTSC magnetic fields B_0 , NSM and MQM sensitivities due to spin projection, transition magnetic dipole moment $\langle f|\mu_z|i\rangle$, largest eigenvalue magnitude of the quadratic Zeeman shift tensor $\lambda_{\text{max}}(\mathbf{K})$, and calculated coherence time T_2 for the example of $^{167}\text{Er}:\text{YSO}$.

Transition	f_0 (MHz)	B_0 (T)	$\Delta\langle \hat{I} \cdot \hat{n} \rangle$	$\Delta\langle S_i n_j I_{ij} \rangle$	$\langle f \mu_z i\rangle$ (MHz / T)	$\lambda_{\text{max}}(\mathbf{K})$ (GHz / T ²)	T_2 (ms)
$ 2\rangle \rightarrow 12\rangle$	3784	0.265	-0.58	-0.09	70	148	34
$ 3\rangle \rightarrow 13\rangle$	3869	0.188	0.38	-0.01	23	137	36
$ 4\rangle \rightarrow 7\rangle$	2226	1.343	-0.47	-0.13	11	35	142
$ 4\rangle \rightarrow 12\rangle$	3145	0.324	0.22	-0.05	174	392	13
$ 5\rangle \rightarrow 7\rangle$	1490	1.160	-0.35	-0.13	158	53	95
$ 6\rangle \rightarrow 7\rangle$	754	1.019	-0.19	-0.09	361	139	36

[1] D. DeMille, J. M. Doyle, and A. O. Sushkov, Probing the frontiers of particle physics with tabletop-scale experiments, *Science* **357**, 990 (2017).

[2] J. T. Singh, A new concept for searching for time-reversal symmetry violation using Pa-229 ions trapped in optical crystals, *Hyperfine Interactions* **240**, 29 (2019).

[3] V. V. Flambaum and V. A. Dzuba, Electric dipole moments of atoms and molecules produced by enhanced nuclear Schiff moments, *Phys. Rev. A* **101**, 042504 (2020).

[4] H. D. Ramachandran and A. C. Vutha, Nuclear T-violation search using octopole-deformed nuclei in a crystal, *Phys. Rev. A* **108**, 012819 (2023).

[5] I. M. Morris, K. Klink, J. T. Singh, J. L. Mendoza-Cortes, S. S. Nicley, *et al.*, Rare isotope-containing diamond colour centres for fundamental symmetry tests, *Philos. Trans. R. Soc. A* **382**, 20230169 (2024).

[6] B. Nima, M. Fan, A. Radak, A. M. Jayich, and A. Vutha, Precision comagnetometry for T-violation searches in crystals, *Phys. Rev. A* **112**, L030801 (2025).

[7] M. Fan, B. Nima, A. Radak, G. Alonzo-Álvarez, and A. Vutha, Wideband search for axionlike dark matter using octupolar nuclei in a crystal, *Phys. Rev. Lett.* **10.1103/dm9j-9pry** (2026).

[8] R. Macfarlane and R. Shelby, Coherent Transient and Holeburning Spectroscopy of Rare Earth Ions in Solids, in *Modern Problems in Condensed Matter Sciences*, Vol. 21 (Elsevier, 1987) pp. 51–184.

[9] V. V. Flambaum and A. J. Mansour, Enhanced magnetic quadrupole moments in nuclei with octupole deformation and their CP-violating effects in molecules, *Phys. Rev. C* **105**, 065503 (2022).

[10] F. Dalton, V. V. Flambaum, and A. J. Mansour, Enhanced Schiff and magnetic quadrupole moments in deformed nuclei and their connection to the search for axion dark matter, *Phys. Rev. C* **107**, 035502 (2023).

[11] M. J. Klein, On a Degeneracy Theorem of Kramers, *Am. J. Phys.* **20**, 65 (1952).

[12] M. Afzelius, M. U. Staudt, H. De Riedmatten, N. Gisin, O. Guillot-Noël, *et al.*, Efficient optical pumping of Zeeman spin levels in $\text{Nd}^{3+}:\text{YVO}_4$, *J. Lumin.* **130**, 1566 (2010).

[13] A. Tiranov, A. Ortu, S. Welinski, A. Ferrier, P. Goldner, *et al.*, Spectroscopic study of hyperfine properties in $^{171}\text{Yb}^{3+}:\text{Y}_2\text{SiO}_5$, *Phys. Rev. B* **98**, 195110 (2018).

[14] S.-J. Wang, Y.-H. Chen, J. J. Longdell, and X. Zhang, Hyperfine states of erbium doped yttrium orthosilicate for long-coherence-time quantum memories, *J. Lumin.* **262**, 119935 (2023).

[15] V. Flambaum, I. Khriplovich, and O. Sushkov, On the P- and T-nonconserving nuclear moments, *Nucl. Phys. A* **449**, 750 (1986).

[16] A. Vutha, What is a Schiff moment anyway?, *arXiv:2601.07217* (2026).

[17] V. Flambaum, D. DeMille, and M. Kozlov, Time-Reversal Symmetry Violation in Molecules Induced by Nuclear Magnetic Quadrupole Moments, *Phys. Rev. Lett.* **113**, 103003 (2014).

[18] E. Fraval, M. J. Sellars, and J. J. Longdell, Method of extending hyperfine coherence times in $\text{Pr}^{3+}:\text{Y}_2\text{SiO}_5$, *Phys. Rev. Lett.* **92**, 077601 (2004).

[19] M. Rančić, M. P. Hedges, R. L. Ahlefeldt, and M. J. Sellars, Coherence time of over a second in a telecom-compatible quantum memory storage material, *Nat. Phys.* **14**, 50 (2018).

[20] K. Matsuura, S. Yasui, R. Kaji, H. Sasakura, T. Tawara,

- et al.*, Exploration of optimal hyperfine transitions for spin-wave storage in $^{167}\text{Er}^{3+}:\text{Y}_2\text{SiO}_5$, arXiv:2412.10126 (2024).
- [21] Y. Takahashi, C. Zhang, A. Jadbabaie, and N. R. Hut-
tler, Engineering Field-Insensitive Molecular Clock Tran-
sitions for Symmetry Violation Searches, *Phys. Rev. Lett.*
131, 183003 (2023).
- [22] Y. Takahashi, H. D. Ramachandran, A. Jadbabaie,
Y. Zeng, C. Zhang, *et al.*, Engineered molecu-
lar clock transitions for symmetry violation searches,
arXiv:2508.06787 (2025).
- [23] T. Böttger, C. W. Thiel, R. L. Cone, and Y. Sun, Con-
trolled compositional disorder in $\text{Er}^{3+}:\text{Y}_2\text{SiO}_5$ provides
a wide-bandwidth spectral hole burning material at 1.5
 μm , *Phys. Rev. B* **77**, 155125 (2008).
- [24] P. Klinkenberg and R. Lang, The spectrum of trebly ion-
ized thorium, Th IV, *Physica* **15**, 774 (1949).
- [25] M. Karbowiak and J. Drożdżyński, Spectral intensities
of U^{3+} ions doped in LaCl_3 single crystals, *Mol. Phys.*
101, 971 (2003).
- [26] B. R. Judd, Optical Absorption Intensities of Rare-Earth
Ions, *Phys. Rev.* **127**, 750 (1962).
- [27] G. S. Ofelt, Intensities of Crystal Spectra of Rare-Earth
Ions, *J. Chem. Phys.* **37**, 511 (1962).
- [28] R. Elwell, C. Schneider, J. Jeet, J. Terhune, H. Morgan,
et al., Laser Excitation of the $^{229\text{m}}\text{Th}$ Nuclear Isomeric
Transition in a Solid-State Host, *Phys. Rev. Lett.* **133**,
013201 (2024).
- [29] J. Tiedau, M. Okhapkin, K. Zhang, J. Thielking,
G. Zitzer, *et al.*, Laser Excitation of the Th-229 Nucleus,
Phys. Rev. Lett. **132**, 182501 (2024).
- [30] C. Zhang, T. Ooi, J. S. Higgins, J. F. Doyle, L. Von
Der Wense, *et al.*, Frequency ratio of the $^{229\text{m}}\text{Th}$ nuclear
isomeric transition and the ^{87}Sr atomic clock, *Nature*
633, 63 (2024).
- [31] K. Beeks, T. Sikorsky, F. Schaden, M. Pressler, F. Schnei-
der, *et al.*, Optical transmission enhancement of ionic
crystals via superionic fluoride transfer: Growing VUV-
transparent radioactive crystals, *Phys. Rev. B* **109**,
094111 (2024).
- [32] Y. Alizadeh, J. Martin, M. Reid, and J.-P. Wells, Intra-
and inter-configurational electronic transitions of Ce^{3+} -
doped Y_2SiO_5 : Spectroscopy and crystal field analysis,
Opt. Mater. **117**, 111114 (2021).
- [33] Y. Alizadeh, J.-P. Wells, M. Reid, A. Ferrier, and
P. Goldner, Laser site-selective spectroscopy of Nd^{3+} -
doped Y_2SiO_5 , *J. Lumin.* **234**, 117959 (2021).
- [34] J. Wittke, Z. Kiss, R. Duncan, and J. McCormick,
Uranium-doped calcium fluoride as a laser material,
Proc. IEEE **51**, 56 (1963).
- [35] M. Louis, E. Simoni, S. Hubert, and J. Gesland, Reduc-
tion by γ -irradiation of tetravalent uranium in LiYF_4 : U
crystals for laser application, *Opt. Mater.* **4**, 657 (1995).
- [36] L. Van Pieterse, M. F. Reid, R. T. Wegh, S. Soverna,
and A. Meijerink, $4f^n \rightarrow 4f^{n-1}5d$ transitions of the light
lanthanides: Experiment and theory, *Phys. Rev. B* **65**,
045113 (2002).
- [37] R. Kumar and D. Joseph, Spectroscopic studies of
Eu doped CaF_2 single crystal, *Mater. Today: Proc.*,
S2214785324003183 (2024).
- [38] A. Lyberis, A. J. Stevenson, A. Sukanuma, S. Ricaud,
F. Druon, *et al.*, Effect of Yb^{3+} concentration on optical
properties of $\text{Yb}:\text{CaF}_2$ transparent ceramics, *Opt. Mater.*
34, 965 (2012).
- [39] J. P. Sattler and J. Nemanich, Electron-Paramagnetic-
Resonance Spectra of Nd^{3+} , Dy^{3+} , Er^{3+} , and Yb^{3+} in
Lithium Yttrium Fluoride, *Phys. Rev. B* **4**, 1 (1971).
- [40] F. Chiossi, E. Lafitte-Houssat, A. Ferrier, S. Welinski,
L. Morvan, *et al.*, Optical coherence and spin population
dynamics in $^{171}\text{Yb}^{3+}:\text{Y}_2\text{SiO}_5$ single crystals, *Phys. Rev.*
B 109, 094114 (2024).
- [41] V. Singh, A. Prasad, M. Seshadri, S. Kaur, and A. S.
Rao, Radiative properties of green-emitting Ho^{3+} doped
 Y_2SiO_5 system: exploring the potential use as a phos-
phor, *J. Mater. Sci.: Mater. Electron.* **34**, 2304 (2023).
- [42] M. Lovrić, P. Glasenapp, and D. Suter, Spin Hamilto-
nian characterization and refinement for $\text{Pr}^{3+}:\text{YAlO}_3$ and
 $\text{Pr}^{3+}:\text{Y}_2\text{SiO}_5$, *Phys. Rev. B* **85**, 014429 (2012).
- [43] B. Lauritzen, N. Timoney, N. Gisin, M. Afzelius,
H. De Riedmatten, *et al.*, Spectroscopic investigations of
 $\text{Eu}^{3+}:\text{Y}_2\text{SiO}_5$ for quantum memory applications, *Phys.*
Rev. B **85**, 115111 (2012).
- [44] T. Chen, C. Zhang, L. Cheng, K. B. Ng, S. Malbrunot-
Ettenauer, *et al.*, Relativistic Exact Two-Component
Coupled-Cluster Study of Molecular Sensitivity Factors
for Nuclear Schiff Moments, *J. Phys. Chem. A* **128**, 6540
(2024).
- [45] L. Cheng, private communication.
- [46] B. Graner, Y. Chen, E. G. Lindahl, and B. R. Heckel, Re-
duced Limit on the Permanent Electric Dipole Moment
of ^{199}Hg , *Phys. Rev. Lett.* **116**, 161601 (2016).
- [47] C. Abel, S. Afach, N. Ayres, C. Baker, G. Ban, *et al.*,
Measurement of the Permanent Electric Dipole Moment
of the Neutron, *Phys. Rev. Lett.* **124**, 081803 (2020).
- [48] I. Schulthess, E. Chanel, A. Fratangelo, A. Gottstein,
A. Gsponer, *et al.*, New Limit on Axionlike Dark Mat-
ter Using Cold Neutrons, *Phys. Rev. Lett.* **129**, 191801
(2022).
- [49] C. Abel, N. Ayres, G. Ban, G. Bison, K. Bodek, *et al.*,
Search for Axionlike Dark Matter through Nuclear Spin
Precession in Electric and Magnetic Fields, *Phys. Rev. X*
7, 041034 (2017).
- [50] C. O'Hare, cajohare/axionlimits: Axionlimits (2020).
- [51] M. Zhong, M. P. Hedges, R. L. Ahlefeldt, J. G.
Bartholomew, S. E. Beavan, *et al.*, Optically addressable
nuclear spins in a solid with a six-hour coherence time,
Nature **517**, 177 (2015).
- [52] T. Böttger, Y. Sun, C. W. Thiel, and R. L. Cone, Spec-
troscopy and dynamics of $\text{Er}^{3+}:\text{Y}_2\text{SiO}_5$ at 1.5 μm , *Phys.*
Rev. B **74**, 075107 (2006).